

## Crystal structure and low-temperature methyl-group dynamics of cobalt and nickel acetates

B. Nicolai, G. J. Kearley, M. R. Johnson, F. Fillaux, and E. Suard

Citation: *J. Chem. Phys.* **109**, 9062 (1998); doi: 10.1063/1.477577

View online: <http://dx.doi.org/10.1063/1.477577>

View Table of Contents: <http://jcp.aip.org/resource/1/JCPSA6/v109/i20>

Published by the AIP Publishing LLC.

### Additional information on J. Chem. Phys.

Journal Homepage: <http://jcp.aip.org/>

Journal Information: [http://jcp.aip.org/about/about\\_the\\_journal](http://jcp.aip.org/about/about_the_journal)

Top downloads: [http://jcp.aip.org/features/most\\_downloaded](http://jcp.aip.org/features/most_downloaded)

Information for Authors: <http://jcp.aip.org/authors>

## ADVERTISEMENT

**physicstoday**

Comment on any  
*Physics Today* article.

**Measured energy in Japan**  
David von Seggern  
(vonseg@seismo.unr.edu) University of Nevada  
July 2012, page 10  
DIGITAL OBJECT IDENTIFIER  
<http://dx.doi.org/10.1063/PT.3.1619>

**Comment on this article**  
By the act of hitting a ball with a bat, one calculates the force energy to deliver the ball to its new location, but one must also take into account that the ball extended its energy to the struck team, which became struck by the ball as its momentum ceased and passed energy to the struck team. Therefore the parameters of the damage extend into the future when the received energy to that pushed upon, later becomes released in a new event. Perhaps calculations of one added that in, while another's calculations did not. E.M.C.  
Written by Edgar McCarvill, 14 July 2012 19:59

# Crystal structure and low-temperature methyl-group dynamics of cobalt and nickel acetates

B. Nicolai, G. J. Kearley, and M. R. Johnson  
*ILL, BP 156, 38042 Grenoble, Cedex 09, France*

F. Fillaux  
*LASIR-CNRS, 2 rue Henry-Dunant, 94320 Thiais, France*

E. Suard  
*ILL, BP 156, 38042 Grenoble, Cedex 09, France*

(Received 22 June 1998; accepted 11 August 1998)

The crystal structures of cobalt and nickel acetate tetrahydrate have been determined at room-temperature and liquid-helium temperature by neutron powder diffraction of the fully deuterated salts. Molecular mechanics and *ab initio* methods based on these structural results have then been used to calculate the rotational potentials experienced by the methyl groups. We have also used inelastic neutron scattering to measure the rotational potential via the rotational tunneling spectrum of the methyl groups, and this has enabled us to compare different methods for the calculation of partial charges in these ionic compounds. Good agreement between the observables and calculations has been obtained for both compounds when *ab initio* methods are used to recalculate partial charges at every step of the methyl rotation. © 1998 American Institute of Physics. [S0021-9606(98)00743-0]

## I. INTRODUCTION

Quantum rotational dynamics of methyl groups at low temperature is well known as a highly sensitive probe of local potentials in molecular crystals. In the present paper we are interested in using this sensitivity to investigate the determination of partial charges within the monopole approximation. Provided that the rotational barrier is not too high (less than about 50 meV), the rotational dynamics are measurable with inelastic neutron scattering (INS) which provides a direct observation of the transitions between tunnel-split librational levels at low temperature. Usually, a single low-energy transition is observed which arises from the librational ground-state splitting. Where there are several types of methyl group, one transition is observed for each crystallographically distinct rotor, each transition being amenable to the single-particle approach.<sup>1</sup> Cobalt and nickel acetates are isostructural and contain a single type of methyl group, but nevertheless, both salts show three spectral peaks in the energy region where methyl tunneling is normally observed. For the purposes of studying partial charges, this apparent complication is unfortunate, but as we will show in both salts that there is in fact a single type of methyl group which gives rise to a single tunneling transition.

Several efforts have been made to correlate the potentials extracted from tunneling spectra with structural data, in order to extract dynamical information. This has been achieved via *ab initio* and molecular-mechanics calculations with various pair potentials (nitromethane,<sup>2,3</sup> acetophenone,<sup>4</sup> acetamide,<sup>5</sup> *p*-xylene,<sup>6</sup> diacetyl,<sup>7</sup> halogenomesitylenes,<sup>8</sup> Hofmann clathrates,<sup>9</sup> aspirin,<sup>10</sup> acetic acid,<sup>11</sup> a series of organic molecules,<sup>12</sup> 2,6 dimethylpyrazine,<sup>13,14</sup> lithium acetate<sup>15</sup>). The most recent investigations<sup>10-15</sup> show clearly that good

agreement can often be achieved, but accurate structural data must be available for the crystal at the same temperature as the tunneling measurements.

The total rotational potential of a methyl group in a crystal can be regarded as the sum of an intramolecular interaction (the rotational potential of an isolated molecule), van der Waals and electrostatic interactions. Although many of the molecules cited above contain polar or ionic groups, the electrostatic part only plays a role in the rotational dynamics of the methyl group when it changes as a function of methyl orientation. Frequently, Coulomb terms are high but virtually unchanged by the methyl orientation, and in a few cases reasonable results have been achieved even when partial charges have been totally neglected.<sup>6-8</sup>

In the published molecular-mechanics work relating to methyl tunneling, the electrostatic interactions have been determined within the monopole approximation, that is point charges centered on the nuclei. The values of these charges can be determined by theoretical or empirical methods, and in systems where the Coulomb energy is sensitive to methyl orientation, it can be difficult to obtain agreement between calculation and experiment. Metal acetates are ideal systems for studying the use of partial charges since they are ionic, cover a wide variety of structural classes, and display methyl tunnelling in a frequency range that is accessible to INS. We start from the premise that knowing of the low-temperature crystal structures, we can confidently calculate the internal and van der Waals contributions to the rotational potential. Any discrepancy between this calculated potential and that measured by INS is due to Coulomb terms and we can use this difference to examine the effects of the partial-charge distributions by applying a series of models to the cobalt and nickel salt.

We have redetermined the room-temperature crystal structures of these acetates using neutron powder diffraction in order to locate the hydrogen (deuterium) atoms. We have also determined the crystal structures at 4 K and found that there is no phase transition on cooling from room temperature, and that the structures contain a single type of methyl group.

## II. EXPERIMENT

The intense red crystals of  $\text{Co}(\text{CH}_3\text{COO})_2 \cdot 4\text{H}_2\text{O}$  were prepared by recrystallization from  $\text{H}_2\text{O}$  of the commercially available product (Prolabo). Samples of  $\text{Co}(\text{CD}_3\text{COO})_2 \cdot 4\text{D}_2\text{O}$  were prepared via the reaction of cobalt carbonate with deuterated acetic acid in  $\text{D}_2\text{O}$  and purified by recrystallization from  $\text{D}_2\text{O}$ . Similarly, the green crystalline samples of nickel acetate were prepared via the reaction of the nickel carbonate with acetic acid and recrystallized from water.

For the INS experiments, the hydrogenous polycrystalline samples were placed in thin-walled aluminium containers which were then placed in a standard liquid-helium cryostat with the sample temperature being controlled at 2 K. The low-energy tunneling spectra were recorded using the IN16 backscattering spectrometer in its high-intensity configuration [unpolished Si(111) analyzers] which gave a resolution of  $1.2 \mu\text{eV}$  [at full width at half maximum (FWHM)]. Tunneling spectra at higher energy were recorded using the time-of-flight spectrometer IN5 with incident wavelengths of 8.81 and  $5.00 \text{ \AA}$  giving resolutions of 19 and  $104 \mu\text{eV}$ , respectively. Librational spectra were also obtained using IN5 but with an incident wavelength of  $2.0 \text{ \AA}$  which gave a resolution of  $1.63 \text{ meV}$ . Vibrational spectra were obtained using the IN1 beryllium-filter spectrometer, which has a resolution of about  $7 \text{ meV}$  ( $60 \text{ cm}^{-1}$ ) in the spectral region of interest, and the TFXA spectrometer with a resolution equal to 1.5% of the energy transfer.

For the diffraction measurements, the deuterated compounds were sealed in thin-walled vanadium containers and maintained at room temperature and liquid-helium temperature using a standard cryostat. The neutron powder-diffraction patterns were obtained using the D1A diffractometer at a fixed neutron wavelength of  $1.909 \text{ \AA}$ . Rietveld refinement of the patterns was achieved using the GSAS program.<sup>16</sup>

## III. DESCRIPTION AND DISCUSSION OF THE STRUCTURE

Cobalt and nickel acetate tetrahydrate crystalline structures were originally determined by x-ray diffraction at room temperature.<sup>17,18</sup> They were found to be isostructural with the space group  $P2_1/c$  and  $Z=2$ . Our work confirmed the essential features of the room-temperature structure and located the deuterium atoms. The calculated densities of  $1.79$  and  $1.80 \text{ g/cm}^3$  for the cobalt salt and the nickel salt, agree well with the measured values:  $1.71$  and  $1.79 \text{ g/cm}^3$ , respectively. There is a single type of acetate group, a single metal atom, but two crystallographically distinct water molecules.

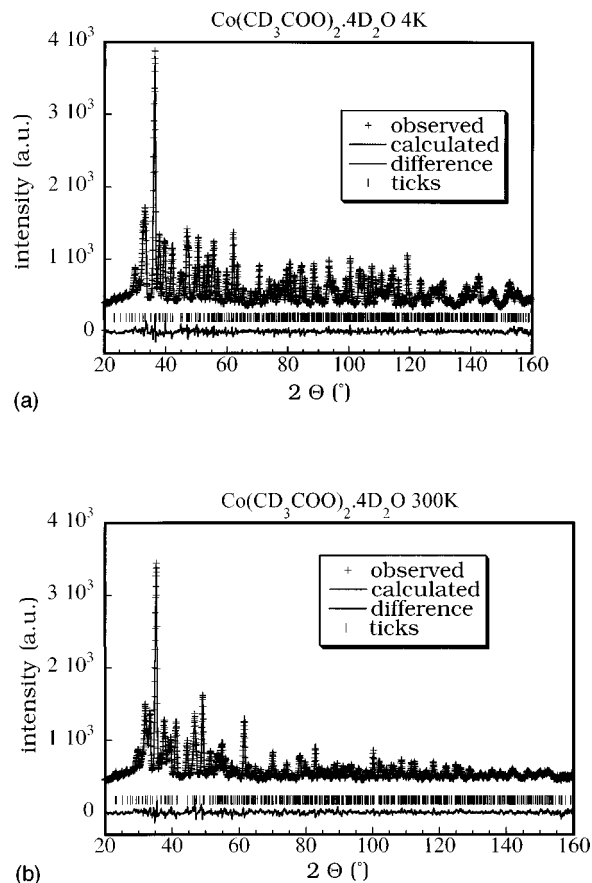


FIG. 1. (a), (b) Observed (crosses), calculated (line) and difference (lower line) diffraction patterns for  $\text{Co}(\text{CD}_3\text{COO})_2 \cdot 4\text{D}_2\text{O}$  at room temperature and at 4 K. The vertical lines mark the positions of Bragg reflections.

On cooling to liquid-helium temperature, we failed to find any structural phase transition, despite previous reports from infrared and Raman investigations.<sup>19,20</sup> The diffraction patterns of the cobalt salt at room temperature and liquid-helium temperature are compared in Figs. 1(a) and 1(b), respectively, with the analogous patterns for the nickel salts in Figs. 2(a) and 2(b). The low-temperature crystal structure of the nickel salt is illustrated in Fig. 2(c), the cobalt being isostructural, and structural data at room and low temperature are collected in Tables I(a) and I(b) (cobalt) and II(a) and II(b) (nickel).

### A. Geometry around the metal atom

Each metal atom is surrounded octahedrally by four water molecules and two oxygen atoms which belong to two different acetate groups. Because the metal atom occupies a center of symmetry at (0,0,0), an octahedron is formed from three symmetry-related pairs of oxygen atoms. The geometry and thermal ellipsoids of the octahedral coordination of the cobalt and the nickel salts are shown in Figs. 3(a) and 3(b), respectively. There is, however, a slight distortion, the metal–oxygen bonds being measurably different (see Table III).

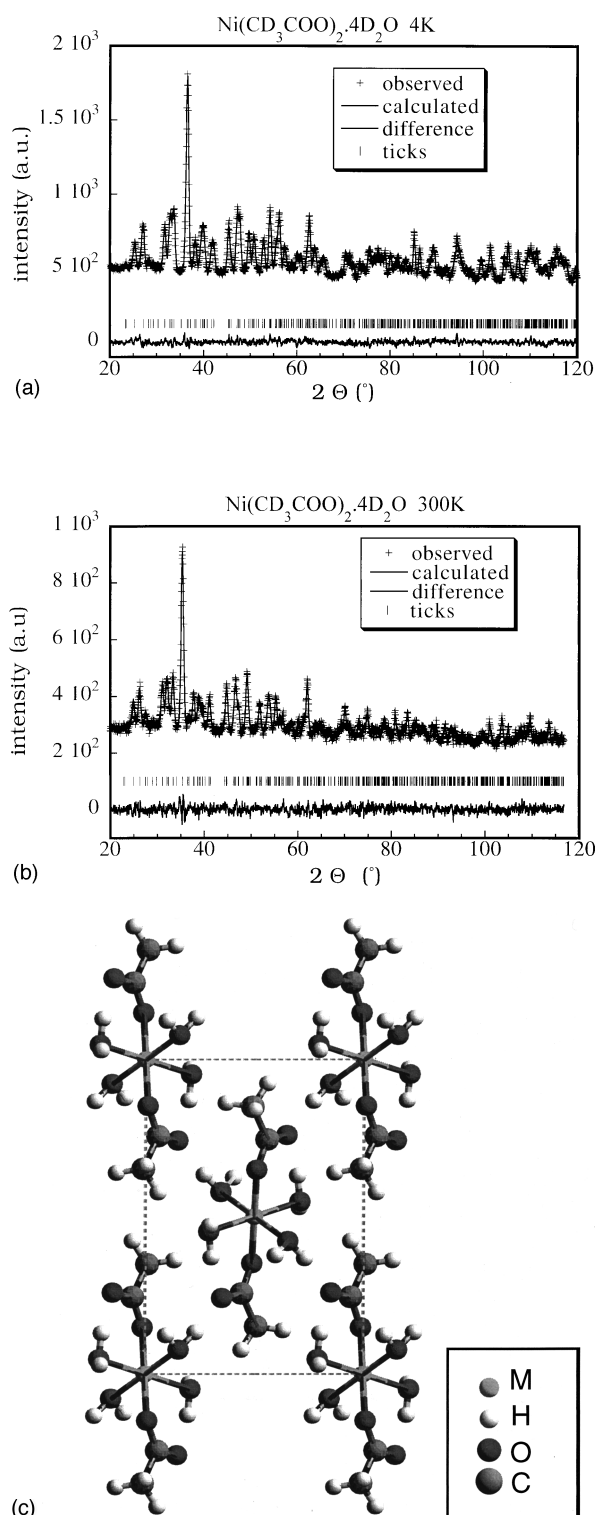


FIG. 2. (a), (b) Observed (crosses), calculated (line), and difference (lower line) diffraction patterns for  $\text{Ni}(\text{CD}_3\text{COO})_2 \cdot 4\text{D}_2\text{O}$  at room temperature and at 4 K. The vertical lines mark the positions of Bragg reflections (c) Illustration of the crystal structure of  $\text{M}(\text{CD}_3\text{COO})_2 \cdot 4\text{D}_2\text{O}$  with  $\text{M}=\text{Co}$  or  $\text{Ni}$  at 4 K.

## B. The acetate group and hydrogen bonding

Within experimental errors, the acetate groups  $\text{C}(7)\text{--}\text{C}(6)\text{--}\text{O}(2)\text{--}\text{O}(3)$  are found to be planar. Parallel sheets of acetate groups [Fig. 2(c)] are generated by the center of sym-

metry at each metal position and a twofold screw axis at  $(1/4)z$ . The acetates are monodentate with only one oxygen atom bonding to the metal atom, the remaining oxygen atom being linked by a hydrogen bond to a water molecule within the same metal coordination group. The two oxygen atoms of an acetate group are linked by hydrogen bonds to water molecules of different groups.

Extensive hydrogen bonding exists. Each acetate is involved in three hydrogen bonds with the surrounding water molecules, and in addition, the water molecules are hydrogen bonded to each other. We note that the thermal ellipsoids of hydrogen atoms in water molecules are almost as large as those of methyl groups at low temperature, as previously found in the lithium acetate dihydrate,<sup>21,15</sup> but again, the water dynamics do not appear to effect the tunneling of the methyl group.

## IV. THE ROTATIONAL POTENTIAL

Coherent rotational tunneling is a phenomenon which occurs in molecular groups whose rotating atoms are indistinguishable such as the hydrogen atoms in a methyl group. The rotational energy levels of a one-dimensional rotor can be obtained by solution of the following Schrödinger equation in the mean-field approach (single-particle model):

$$\left( -\frac{\hbar^2}{2I} + V(\phi) \right) \psi = E\psi, \quad (1)$$

where  $I$  is the moment of inertia of the rotor,  $\phi$  the angular coordinate, and  $V(\phi)$  the local static crystalline rotational potential. In this model, the rotor is symmetric and performs a one-dimensional rigid rotation about its three fold axis. The rotational potential of  $\text{CH}_3$  is periodic and can be expanded in Fourier series as follow:

$$V(\phi) = \sum_n \frac{1}{2} V_{3n} [1 - \cos(3n\phi + \delta_{3n})]. \quad (2)$$

$V_{3n}$  is the amplitude of the  $3n$ -fold contribution and  $\delta_{3n}$  is a phase.<sup>1</sup> For calculation convenience, the expansion is usually truncated to the first or second order.

Each triply degenerate energy level is split into two tunneling states due to the overlap of the wave functions in the adjacent wells:  $A$  states and the doubly degenerate  $E$  states. For simplicity, we distinguish two kinds of transition: tunneling transitions (in the  $\mu\text{eV}$  range) between the tunneling states  $A$  and  $E$  of the librational ground state, and librational transitions (in the  $\text{meV}$  range) between the librational ground state and the first librational excited state. The process is quantum mechanical and at low temperature, (less than about 50 K) the tunneling transitions can be directly measured by INS. Because the tunnel splitting has an approximately exponential dependence on the rotational barrier height, it is extremely sensitive to the molecular crystal potentials.

## V. RESULTS

Incoherent neutron scattering is largely dominated by hydrogen dynamics, the cross section of hydrogen being almost ten times greater than the cross section of other nuclei. Consequently, intense peaks in the 1–600  $\mu\text{eV}$  region of the

TABLE I. Atomic positions, occupancy (occ), and thermal parameters (in  $\text{\AA}^2$ ) (a) for cobalt acetate tetrahydrate at 1.5 K, (b) for cobalt acetate tetrahydrate at 300 K.

Atoms	$x/a$	$y/b$	$z/c$	occ	$U_i/U_e^*100$
(a) $P21/c$ , $a=4.7881(1)$ $\text{\AA}$ , $b=11.8664(3)$ $\text{\AA}$ , $c=8.2376(2)$ $\text{\AA}$ , $\gamma=92.659(2)^\circ$ .					
Co(1)	0.0000(0)	0.0000(0)	0.0000(0)	1	0.03(33)
O(2)	-0.2333(11)	-0.1485(4)	0.0093(6)	1	0.59(11)
O(3)	0.0820(8)	-0.2587(4)	0.1484(5)	1	0.34(11)
O(4)	-0.2838(9)	0.0778(4)	0.1519(6)	1	0.20(11)
O(5)	0.2336(11)	-0.0473(4)	0.2102(6)	1	1.31(12)
C(6)	-0.1326(7)	-0.2445(4)	0.0563(5)	1	0.10(10)
C(7)	-0.2872(9)	-0.3485(4)	-0.0113(5)	1	0.47(11)
D(8)	-0.2271(9)	-0.4231(4)	0.0567(5)	1	2.02(12)
D(9)	-0.5104(10)	-0.3379(4)	-0.0065(5)	1	2.38(12)
D(10)	-0.2319(9)	-0.3609(4)	-0.1335(6)	1	2.50(12)
D(11)	0.4341(10)	-0.0249(4)	0.2081(6)	1	2.09(13)
D(12)	-0.4414(9)	0.1233(4)	0.0933(5)	1	1.40(12)
D(13)	0.2219(8)	-0.1302(4)	0.1991(5)	1	1.59(13)
D(14)	-0.2044(9)	0.1329(4)	0.2293(5)	1	1.24(12)
(b) $P21/c$ , $a=4.8214(2)$ $\text{\AA}$ , $b=11.9633(4)$ $\text{\AA}$ , $c=8.4525(4)$ $\text{\AA}$ , $\gamma=94.247(3)^\circ$ .					
Co(1)	0.0000	0.0000	0.0000	1	0.7(5)
O(2)	-0.2260(20)	-0.1422(7)	0.0100(11)	1	4.73(23)
O(3)	0.0737(14)	-0.2563(7)	0.1559(8)	1	3.71(21)
O(4)	-0.2764(17)	0.0848(6)	0.1533(10)	1	4.02(25)
O(5)	0.2461(17)	-0.0475(6)	0.2147(9)	1	3.27(23)
C(6)	-0.1390(11)	-0.2413(5)	0.0654(6)	1	1.68(16)
C(7)	-0.3013(17)	-0.3438(6)	0.0023(9)	1	3.14(18)
D(8)	-0.2562(26)	-0.4117(9)	0.0698(11)	1	9.80(32)
D(9)	-0.5090(26)	-0.3323(9)	-0.0012(12)	1	11.98(45)
D(10)	-0.2308(19)	-0.3586(9)	-0.1061(12)	1	9.18(33)
D(11)	0.4434(18)	-0.0280(7)	0.1926(10)	1	6.40(28)
D(12)	-0.4341(15)	0.1234(7)	0.0893(9)	1	5.90(26)
D(13)	0.2188(17)	-0.1288(7)	0.1962(10)	1	6.47(28)
D(14)	-0.1917(15)	0.1340(6)	0.2240(8)	1	3.89(21)

als are normally attributed to rotational tunneling. However, in the case of cobalt and nickel acetates tetrahydrate, the low-temperature crystal structure shows clearly a unique type of methyl group, which is in conflict with the presence of three peaks due to tunneling. We will now look into the tunneling spectra in more detail.

### A. Tunneling spectra of cobalt acetate tetrahydrate

A neutron-transmission measurement of cobalt acetate tetrahydrate predicts three distinct tunneling peaks at 1.1, 30, and 47  $\mu\text{eV}$  (0.012, 0.35, and 0.55 K).<sup>22</sup> The INS spectra of the commercially available product of the cobalt salt, without further purification, show clearly three inelastic peaks: at 30 and 5  $\mu\text{eV}$  using IN5, and a third at 1.2  $\mu\text{eV}$  using IN16 [Figs. 4(a) and 4(b), respectively]. Although these observations are in good agreement with the transmission measurements above, Guckelsberger *et al.*<sup>22</sup> pointed out that their results depended on sample preparation. A careful examination of commercial cobalt acetate tetrahydrate reveals a mixture of different types of crystals. After a simple recrystallization from water, the peaks on the IN5 spectrum vanish, and only the single peak in the IN16 spectrum at 1.2  $\mu\text{eV}$  remains. This peak corresponds to the expected tunneling of the crystallographically unique methyl group and the two extra peaks probably arise from cobalt acetate hydrate with less than four water molecules. A full characterization of these hydrates is beyond the scope of the present paper.

### B. Tunneling spectra of nickel acetate tetrahydrate

Previous INS measurements of nickel acetate tetrahydrate on IN10 revealed a unique tunneling peak at 1.4  $\mu\text{eV}$ ,<sup>23</sup> but there seems to have been no attempt to search for peaks beyond the range of this spectrometer (14  $\mu\text{eV}$ ). Our spectra of the nickel salt exhibit three peaks: the previously measured 1.4  $\mu\text{eV}$  on IN16, and two additional peaks at 320 and 710  $\mu\text{eV}$  on IN5 [Figs. 5(a) and 5(b), respectively]. However, we found that peaks at 320 and 710  $\mu\text{eV}$  are virtually unchanged by deuteration of the methyl group [Fig. 5(c)], so we attribute these peaks to magnetic transitions. It transpires that these transitions correspond remarkably well with those predicted at 330 and 700  $\mu\text{eV}$  by previous magnetic susceptibility measurements on this salt at liquid-helium temperature.<sup>24–26</sup>

### C. Librational spectra

Both acetates show a single tunneling transition close to 1.5  $\mu\text{eV}$ , with the additional peaks being due to partially hydrated species in the cobalt salt, and magnetic transitions in the nickel salt. Correspondingly, we anticipate a single librational transition which will provide further information on the rotational potential. Librational spectra were recorded on IN5 with an incident wavelength of 2  $\text{\AA}$  and are shown in Figs. 6(a) and 6(b), respectively. In both cases there is an intense peak close to 15 meV, with weaker features at about

TABLE II. Atomic positions, occupancy (occ), and thermal parameters (in  $\text{\AA}^2$ ) (a) for nickel acetate tetrahydrate at 1.5 K, (b) for nickel acetate tetrahydrate at 300 K.

Atoms	$x/a$	$y/b$	$z/c$	occ	$U_i/U_e^*100$
(a) $P21/c$ , $a=4.7485 \text{ \AA}$ , $b=11.6933 \text{ \AA}$ , $c=8.2247 \text{ \AA}$ , $\gamma=92.524^\circ$ .					
Ni(1)	0.0000(0)	0.0000(0)	0.0000(0)	1	0.33
O(2)	-0.2386	-0.1518	0.0103	1	0.11
O(3)	0.0821	-0.2598	0.1434	1	0.79
O(4)	-0.2866	0.0794	0.1499	1	0.94
O(5)	0.2357	-0.1497	0.2058	1	1.00
C(6)	-0.1346	-0.2440	0.0526	1	0.03
C(7)	-0.2913	-0.3517	-0.0162	1	1.00
D(8)	-0.2227	-0.4278	0.0528	1	1.74
D(9)	-0.5177	-0.3397	-0.0091	1	2.42
D(10)	-0.2316	-0.3655	-0.1395	1	2.47
D(11)	0.4271	-0.0255	0.2020	0.62	2.35
D(12)	-0.4311	0.1223	0.0963	0.58	1.35
D(13)	0.2238	-0.1315	0.1967	0.56	0.75
D(14)	-0.1936	0.1308	0.2323	0.52	0.33
(b) $P21/c$ , $a=4.7769 \text{ \AA}$ , $b=11.7809 \text{ \AA}$ , $c=8.4171 \text{ \AA}$ , $\gamma=93.826^\circ$ .					
Ni(1)	0.0000(0)	0.0000(0)	0.0000(0)	1	0.95
O(2)	-0.2413	-0.1552	0.0071	1	2.69
O(3)	0.0799	-0.2541	0.1589	1	2.93
O(4)	-0.2781	0.0810	0.1508	1	1.28
O(5)	0.2312	-0.427	0.2015	1	2.00
C(6)	-0.1412	-0.2439	0.0674	1	1.40
C(7)	-0.2922	-0.3487	-0.0284	1	5.93
D(8)	-0.2521	-0.4125	0.0561	1	8.79
D(9)	-0.4976	-0.3422	0.0035	1	8.71
D(10)	-0.2338	-0.3598	-0.1207	1	20.01
D(11)	0.4234	-0.0349	0.1921	0.62	3.88
D(12)	-0.4331	0.1204	0.0856	0.58	5.18
D(13)	0.2149	-0.1267	0.1973	0.56	2.87
D(14)	-0.1892	0.1299	0.2235	0.52	0.93

10 and 18 meV. We assign the most intense peak to the librations of the methyl groups, which is in accordance with the previous assignment of Clough *et al.* for the nickel salt.<sup>23</sup>

We also recorded the librational spectra of the partially deuterated salts,  $\text{Co}(\text{CH}_3\text{COO})_2 \cdot 4\text{D}_2\text{O}$  and  $\text{Ni}(\text{CH}_3\text{COO})_2 \cdot 4\text{D}_2\text{O}$ , and found these to be very similar to those of the protonated compounds. This suggests that despite the large thermal ellipsoids of the water molecules in the low-temperature crystal structure, the water motions are independent of the methyl groups rotations. A similar observation was made for lithium acetate dihydrate,<sup>15</sup> where there are also large thermal displacements of hydrogen atoms in water molecules at 4 K, but deuteration of the water has no measurable effect on the methyl tunneling.

## VI. THE COMPUTATIONAL METHOD

According to the single-particle model, the rotating methyl group in the unit cell was modeled as a rigid, equilateral triangle of hydrogen atoms. The methyl group was symmetrized as geometric average of crystallographic data (CH lengths, CCH, and HCH angles). This single methyl group was rotated in a stepwise manner, the environment including all other methyl groups was assumed to be static, the atomic positions used being those determined by neutron diffraction at 4 K.

The total rotational barrier  $V_{\text{tot}}$  can be expressed as a function of the rotational angle of the methyl group  $\phi$ :  $V(\phi) = V_{\text{int}}(\phi) + V_{\text{vdW}}(\phi) + V_{\text{Coul}}(\phi)$ , where  $V_{\text{int}}$  is the internal contribution (the barrier of the isolated molecule),  $V_{\text{vdW}}$  is the van der Waals (vdW) contribution, and  $V_{\text{Coul}}$  is the Coulomb contribution. The internal contribution was calculated by *ab initio* methods and the external contribution (van der Waals and electrostatic) by using pair potentials and a variety of partial-charge methods, as in Ref. 11.

### A. Internal barrier

We obtained the internal barrier for the isolated molecule by *ab initio* calculations from the program GAMESS-UK<sup>27</sup> using the Hartree-Fock theory and the self-consistent field method. The only split valence basis set available for first-row transition metal in GAMESS-UK is 3-21G.<sup>28</sup> We used the experimental geometry (bond length, angles, and torsions) as determined by neutron diffraction [see Table III and Figs. 3(a) and 3(b)], and then performed single-point calculations over a number of different rotational conformations of the methyl group about the C-C axis of the acetate group.

### B. External contribution

Molecular mechanics is generally used for the structures and the conformational energies of organic and biological

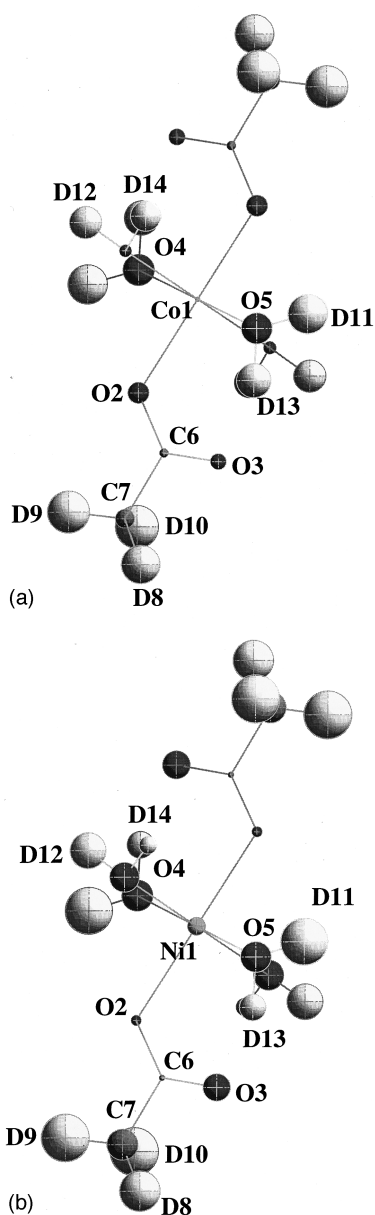


FIG. 3. (a), (b) Illustration of the octahedral symmetry around the metal atom in  $M(\text{CD}_3\text{COO})_2 \cdot 4\text{D}_2\text{O}$ , with  $M=\text{Co}$  and  $M=\text{Ni}$ , respectively, at 4 K showing the thermal ellipsoids.

molecules, there being several specific force fields available. For transition-metal complexes, however, the situation is very different because of the diversity of geometries, coordinations, and oxidation states which can occur. A recent force field, UFF,<sup>29</sup> has been developed which successfully reproduces the structures of variety of metal-containing compounds.<sup>30</sup> We used this empirical force field and the Ewald summation method<sup>31</sup> to calculate the van der Waals (vdW) term by molecular mechanics using the commercial program Cerius<sup>2</sup>.<sup>32</sup>

The expression of the vdW interactions was given by the exponential-6 potential (exp-6):

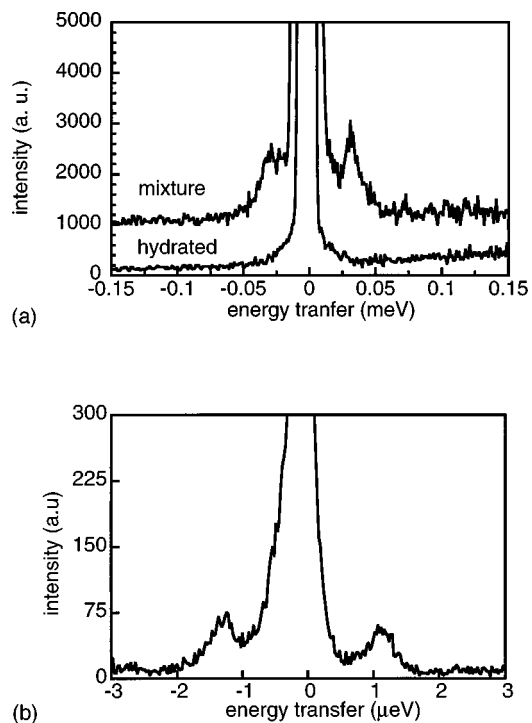


FIG. 4. (a) Inelastic neutron spectrum of  $\text{Co}(\text{CH}_3\text{COO})_2 \cdot 4\text{H}_2\text{O}$  measured on IN5 at 1.5 K, of the commercial mixture and the fully hydrated form. Incident wavelength: 13 Å. The intensities are in arbitrary units (a.u.) (b) Inelastic neutron spectrum of  $\text{Co}(\text{CH}_3\text{COO})_2 \cdot 4\text{H}_2\text{O}$  measured on IN10 at 1.5 K.

$$V_{\text{vdW}} = D_0(i,j) \left( \left[ \left( \frac{6}{\gamma(i,j) - 6} \right) \exp \left[ \gamma(i,j) \left( 1 - \frac{R(i,j)}{R_0(i,j)} \right) \right] - \left[ \left( \frac{\gamma(i,j)}{\gamma(i,j) - 6} \right) \left( \frac{R(i,j)}{R_0(i,j)} \right)^6 \right] \right] \right), \quad (3)$$

where  $R(i,j)$  is the distances between the atoms  $i$  and  $j$ ,  $D_0(i,j)$  the bond strength,  $R_0(i,j)$  the bond length, and  $\gamma(i,j)$  a scaling factor (typically 12).

In some cases, the Coulomb term was also determined with Cerius<sup>2</sup>. Molecular-mechanics methods commonly use the monopole approximation, in which point charges are attributed to atomic positions, whereas in organic nonpolar systems, the electrostatic interactions are small (but not negligible), in ionic or polar molecules, the Coulomb contributions are more important. Unfortunately, it is not possible to derive site charges directly from observables (such as molecular dipole or multipole moments) and it is clear that the neglect of the charges in molecules which are more polar than the hydrocarbons will cause unreliable calculation of equilibrium atomic positions, and potential-energy surfaces.

The Coulomb energy is modeled as follows:

$$V_{\text{Coul}} = \frac{Q_i Q_j}{4\pi\epsilon_0 R(i,j)}, \quad (4)$$

where  $Q_i$  and  $Q_j$  represent the partial charges of the atoms  $i$  and  $j$ , respectively.

These point charges can be obtained by two methods:

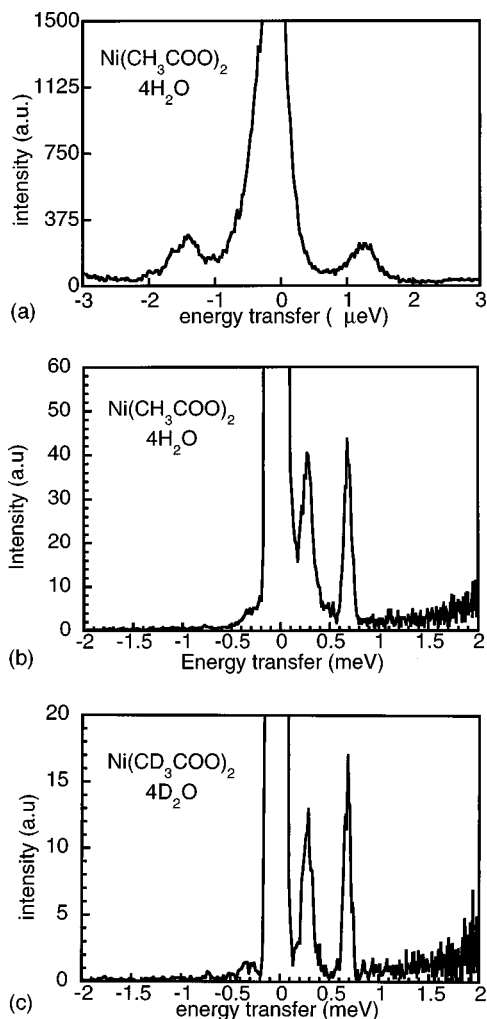


FIG. 5. (a) Inelastic neutron spectrum of  $\text{Ni}(\text{CH}_3\text{COO})_2 \cdot 4\text{H}_2\text{O}$  measured on IN10 at 1.5 K. (b) Inelastic neutron spectrum of  $\text{Ni}(\text{CH}_3\text{COO})_2 \cdot 4\text{H}_2\text{O}$  measured on IN5 at 1.5 K. Incident wavelength: 5 Å. (c) Inelastic neutron spectrum of  $\text{Ni}(\text{CD}_3\text{COO})_2 \cdot 4\text{D}_2\text{O}$  measured on IN5 at 1.5 K. Incident wavelength: 5 Å.

The first method is the empirical  $Q_{\text{eq}}$  charge equilibration, which is based on the geometry of the molecule and experimental atomic properties (atomic ionization potentials, electron affinities, and atomic radii).<sup>33</sup>

The second method is potential-derived charges (PDC) obtained from *ab initio* method: the electrostatic potential is determined for the isolated molecule and the charges at atomic positions are attributed by least-squares fitting to the potential surface.

## VII. CALCULATIONS AND DISCUSSION

So far we have discussed the experimental information concerning the barrier heights and equilibrium methyl conformation. We will now consider the calculated equilibrium orientation, tunneling, and librational frequencies, and compare these with the observed values.

According to the single-particle model [see Eqs. (1) and (2)], the energy barrier as a function of the orientation  $\phi$  of the methyl group can be modeled with the Fourier series of Eq. (2) (with  $n = 3$ ).

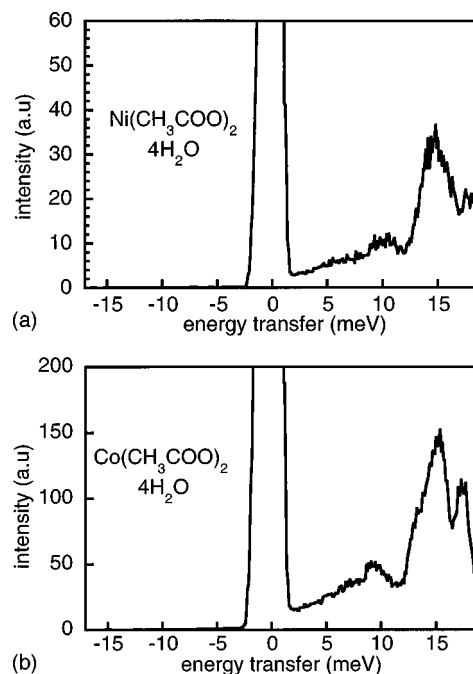


FIG. 6. (a), (b) Librational spectra of  $\text{Ni}(\text{CH}_3\text{COO})_2 \cdot 4\text{H}_2\text{O}$  and  $\text{Co}(\text{CH}_3\text{COO})_2 \cdot 4\text{H}_2\text{O}$ , respectively, measured on IN5 at 1.5 K. Incident wavelength: 2 Å.

Assuming classical mechanics, the position of the atom found by diffraction corresponds to the equilibrium position of this atom in the crystal. Accordingly, we choose the methyl conformation found by neutron diffraction at low temperature as the reference ( $\phi = 0^\circ$ ,  $\delta_n = 0$ ) for the following calculations, which should clearly correspond to the minimum in the calculated rotational barrier in the crystal.

### A. The internal barrier

The model we have chosen for the *ab initio* calculations of the internal barrier is a neutral octahedron comprised of a metal atom surrounded by two crystallographically equivalent acetates and four water molecules [see Table III and Figs. 3(a) and 3(b)]. This model was selected because the electronic distribution in the acetate ion,  $\text{CH}_3\text{COO}^-$ , is expected to be strongly influenced by the covalent-ionic nature of the oxygen-metal bonding.

The Fourier coefficients [Eq. (2)] were found to be  $V_3 = 14.7$  meV for nickel acetate tetrahydrate and  $V_3 = 9.4$  meV for cobalt acetate tetrahydrate, the higher terms being negligibly small. The *ab initio* calculations reveal that the minimum-energy conformation in the isolated molecule does not correspond to the experimental conformation found in the crystal, the minimum being at  $-18^\circ$  for the nickel salt and  $-15^\circ$  for cobalt salt. The *ab initio* conformation corresponds to one methyl H atom being located in the molecular plane of the acetate, which strongly implies that the intermolecular interactions in the crystal distort the free-molecule conformation. A similar result was found for 2,6 dimethylpyrazine, in which the specific conformations of two inequivalent methyl groups arise exclusively from van der Waals and Coulomb interactions in the crystal.<sup>13,14</sup>

TABLE III. Geometry of the asymmetric unit in  $M(\text{CD}_3\text{COO})_2\cdot 4\text{D}_2\text{O}$  with  $M=\text{Co}$ ,  $\text{Ni}$  at 1.5 K and room temperatures, distances are in Å, torsions and angles in degrees.

Atoms	Atoms	M=Co, 1.5 K	M=Ni, 1.5 K	M=Co, 300 K	M=Ni, 300 K
M(1)	O(2)	2.090	2.109	2.025	2.066
C(6)	O(2)	1.289	1.230	1.331	1.344
O(3)	C(6)	1.260	1.258	1.246	1.271
C(7)	C(6)	1.531	1.556	1.529	1.618
D(8)	C(7)	1.079	1.097	1.007	1.043
D(9)	C(7)	1.079	1.088	1.009	1.037
D(10)	C(7)	1.063	1.078	1.016	0.853
O(4)	M(1)	2.103	2.094	2.177	2.124
D(12)	O(4)	1.030	0.943	1.002	1.005
D(14)	O(4)	0.978	0.994	0.913	0.923
O(5)	M(1)	2.094	2.071	2.169	2.025
D(11)	O(5)	0.972	0.954	1.01	0.931
D(13)	O(5)	0.989	0.960	0.992	0.994

Angles			M=Co, 1.5 K	M=Ni, 1.5 K	M=Co, 300 K	M=Ni, 300 K
Atoms	Atoms	Atoms				
M(1)	O(2)	C(6)	124.26	122.65	127.32	122.82
O(3)	C(6)	O(2)	125.60	127.17	124.60	124.86
C(7)	C(6)	O(2)	115.80	115.29	116.85	109.68
D(8)	C(7)	C(6)	111.08	109.99	111.45	98.90
D(9)	C(7)	C(6)	110.85	109.52	112.46	102.27
D(10)	C(7)	C(6)	108.58	108.77	104.92	114.14
O(4)	M(1)	O(2)	89.26	89.17	90.67	88.99
D(12)	O(4)	M(1)	115.53	115.98	110.99	110.38
D(14)	O(4)	M(1)	116.05	112.85	115.21	113.43
O(5)	M(1)	O(2)	90.55	90.17	90.44	92.55
D(11)	O(5)	M(1)	114.23	111.79	104.42	112.94
D(13)	O(5)	M(1)	99.46	100.83	93.84	100.37

Torsions				M=Co, 1.5 K	M=Ni, 1.5 K	M=Co, 300 K	M=Ni, 300 K
Atoms	Atoms	Atoms	Atoms				
M(1)	O(2)	C(6)	O(3)	23.7	25.6	19.1	17.8
C(7)	C(6)	O(2)	O(3)	-178.3	-179.7	-175.1	-165.2
D(8)	C(7)	C(6)	O(2)	-164.8	-164.2	-164.9	-159.8
D(9)	C(7)	C(6)	D(8)	120.7	121.5	120.6	92.6
D(10)	C(7)	C(6)	D(8)	-118.4	-116.0	-115.8	-125.0
O(4)	M(1)	O(2)	C(6)	-123.8	-125.9	-119.3	-118.0
D(12)	O(4)	M(1)	O(2)	-95.3	-95.8	-91.4	-90.7
D(14)	O(4)	M(1)	D(12)	-119.5	-123.8	-125.3	-125.8
O(5)	M(1)	O(2)	O(4)	87.7	89.1	86.9	86.5
D(11)	O(5)	M(1)	O(2)	140.6	145.4	137.7	132.5
D(13)	O(5)	M(1)	D(11)	-111.8	-117.1	-109.9	-105.4

## B. The external contributions

### 1. van der Waals contributions

The vdW contribution can be estimated by summing the pairwise interactions between each of the methyl H atoms and the other atoms in the model. This contribution was found to be  $V_3(\text{vdW})=17.9$  meV, the minimum of the energy being at  $-33^\circ$  for the nickel salt and  $V_3(\text{vdW})=22.4$  meV with the minimum at  $-37^\circ$  for the cobalt salt. The different contributions to the vdW potential can be analysed on an atom-by-atom basis, and this reveals that the contributions of the surrounding metal atoms and the carbon are negligibly small [see Figs. 7(a) and 7(b) for the nickel salt and the cobalt salt, respectively]. It is essential that the contributions from the hydrogen and the oxygen atoms of the surroundings water molecules dominate the van

der Waals contribution to rotational potential, which is similar to results reported for lithium acetate dihydrate.<sup>15</sup>

### 2. Coulomb contributions

The sum of the van der Waals and internal contributions to the rotational barrier is too small to account for the observed tunneling and librational frequencies. Further, the minimum in this rotational potential does not correspond well to the crystallographically determined methyl orientation, and it is clear that Coulomb interactions must play an important role in this crystal. We have tested four models of the charge distributions which are essentially based on two methods of estimating the partial charges of a molecule: em-

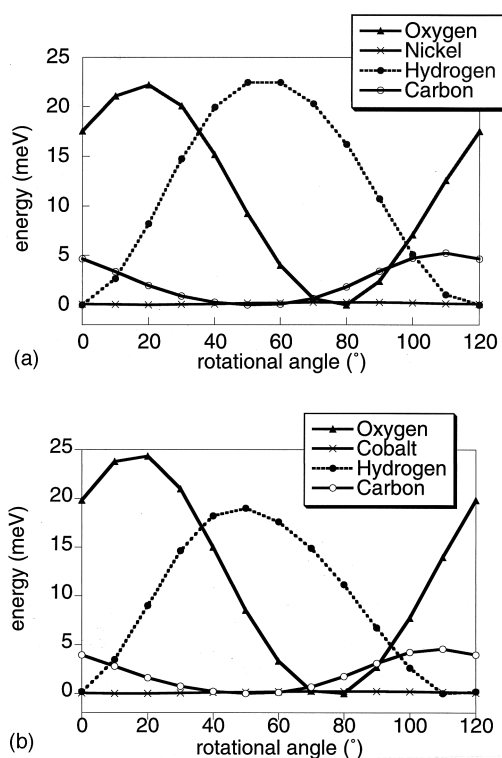


FIG. 7. Contributions of the carbon, metal, oxygen, and hydrogen atoms to the van der Waals component of the rotational potential. Carbon: solid line and an open circle, metal: solid line and a cross, oxygen: solid line and a solid triangle, hydrogen: dotted line with a solid circle. (a) In nickel acetate tetrahydrate, (b) in cobalt acetate tetrahydrate.

pirical calculations with the  $Q_{eq}$  method in the crystal and the potential-derived charges calculated via *ab initio* methods.

*a. The four methods.* (1) In this method, the charges are evaluated with  $Q_{eq}$  for the experimental conformation of the methyl groups, with the point charges being evaluated for the octahedron in the crystal. The charges of the environment and the three H atoms of the probe methyl are constrained to these calculated values during rotation of the methyl group.

(2) Potential-derived charges are evaluated for all the atoms of the octahedron by *ab initio* method. They are transferred in the crystal to obtain to total Coulomb contribution to the potential. As in method 1, the charges of the methyl group and the environment are kept fixed during the rigid rotation of the methyl group, the charges of the three H atoms being averaged.

(3) According to  $Q_{eq}$ , the partial charges depend upon the geometry and consequently upon the conformation of the molecules, the partial charges of the methyl group can vary during the rotation. Consequently, in the third method, we performed a new  $Q_{eq}$  calculation at every step of the rigid rotation of the methyl groups in the crystal.

(4) Because the potential-derived charges are determined from a wave function which depends on the atomic positions, they should be calculated for the isolated octahedron at each step of the rotation and then introduced into the crystal. This method is much more computationally expensive than the preceding three methods.

TABLE IV. Partial charges of the 29 atoms of the octahedron calculated by  $Q_{eq}$  method or *ab initio* method (PDC: potential-derived charges) and used in the calculations of the rotational potential.

Atoms	M=Co, $Q_{eq}$	M=Ni, $Q_{eq}$	M=Ni, PDC
M(1)	0.5892	0.4845	1.1650
O(2)	-0.4589	-0.4579	-0.8304
O(3)	-0.6555	-0.6662	-0.8470
O(4)	-0.7297	-0.7514	-0.8659
O(5)	-0.7417	-0.7556	-0.9670
C(6)	0.6115	0.6373	1.1139
C(7)	-0.3077	-0.3122	-0.6407
H(8)	0.1757	0.1711	0.1589
H(9)	0.1399	0.1520	0.1643
H(10)	0.1620	0.1714	0.1501
H(11)	0.3702	0.3851	0.4672
H(12)	0.3651	0.3846	0.4749
H(13)	0.3930	0.4048	0.4812
H(14)	0.3917	0.3948	0.5563
O(2) bis	-0.4589	-0.4579	-0.8189
O(3) bis	-0.6555	-0.6662	-0.8423
O(4) bis	-0.7297	-0.7514	-0.8610
O(5) bis	-0.7417	-0.7556	-0.9594
C(6) bis	0.6115	0.6373	1.0959
C(7) bis	-0.3077	-0.3122	-0.6407
H(8) bis	0.1757	0.1711	0.1517
H(9) bis	0.1399	0.1520	0.1591
H(10) bis	0.1620	0.1714	0.1463
H(11) bis	0.3702	0.3851	0.4640
H(12) bis	0.3651	0.3846	0.4725
H(13) bis	0.3930	0.4048	0.4820
H(14) bis	0.3917	0.3948	0.5476

*b. Discussion.* The partial charges used for the calculations are presented in Table IV and Fig. 8 and the results of the four methods outlined above are shown in Figs. 9(a)–9(d) for the nickel salt. It can be seen from Table IV that the

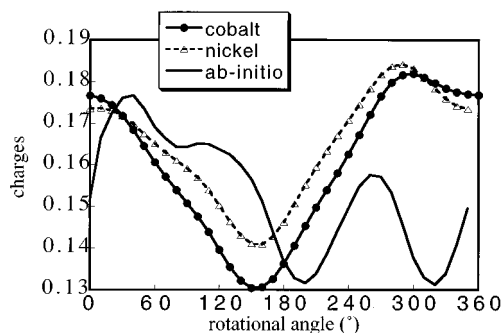


FIG. 8. Partial charges of the hydrogen H(8) of the rotating methyl group calculated by  $Q_{eq}$  method in the cobalt and the nickel salts as a function of the methyl-group orientation angle. Comparison with the partial charges calculated by *ab initio* method. Charges in the cobalt salt calculated with  $Q_{eq}$ : solid line with solid circle. Charges in the nickel salt calculated with  $Q_{eq}$ : dotted line with open triangle. Charges calculated by *ab initio* method: solid line. The minima and maxima are similar in the three cases but the form of curves is different between  $Q_{eq}$  and *ab initio* method. Moreover, in  $Q_{eq}$ , the charges of the H atoms of the methyl group are varied. In *ab initio*, the charge of the carbon atom varies with the charges of the H atoms. The charges of all other atoms are invariant during rotation.

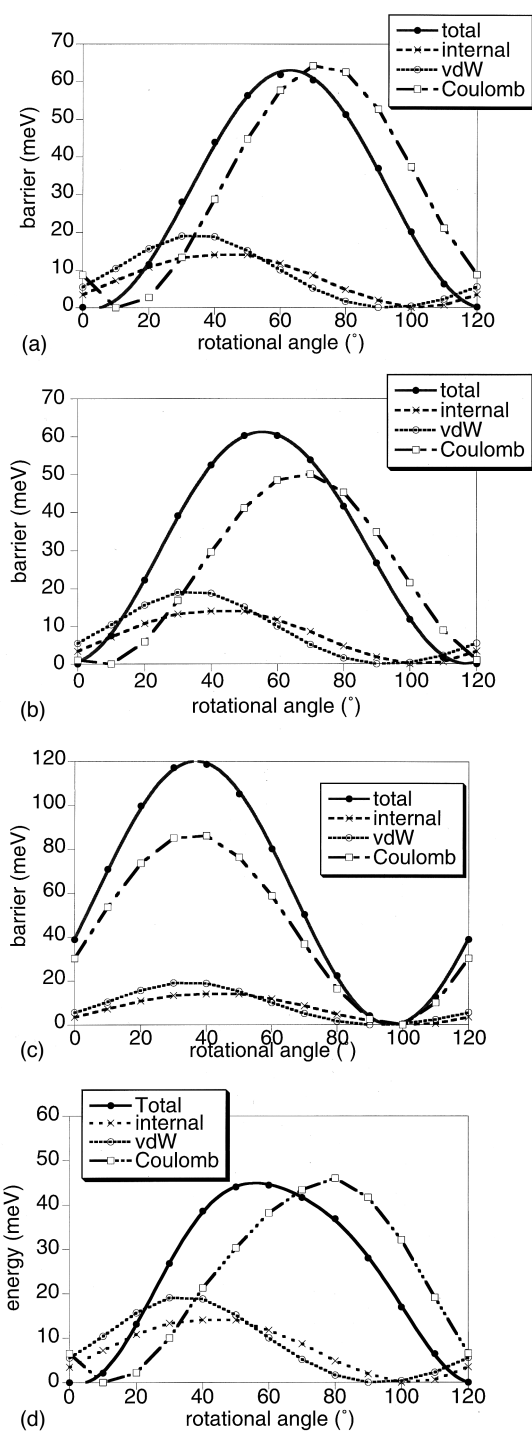


FIG. 9. Calculation of the rotational potential in nickel acetate tetrahydrate. Total potential: solid curve with solid circle, van der Waals: dotted curve with open circle, Coulomb: dashed curve with open square, Internal: dotted curve with a cross. (a) Partial charges are calculated with the  $Q_{eq}$  method and are fixed during the rotation of the methyl group. (b) Partial charges are calculated with *ab initio* method and are fixed during the rotation of the methyl group. (c) Partial charges are calculated with the  $Q_{eq}$  method and vary during the rotation of the methyl group. (d) Partial charges are calculated with *ab initio* method and vary during the rotation of the methyl group.

charges in the cobalt salt and the nickel salt calculated with the empirical  $Q_{eq}$  method are very similar, as expected for such closely related compounds. These charges are, however, very different from those calculated with the *ab initio*

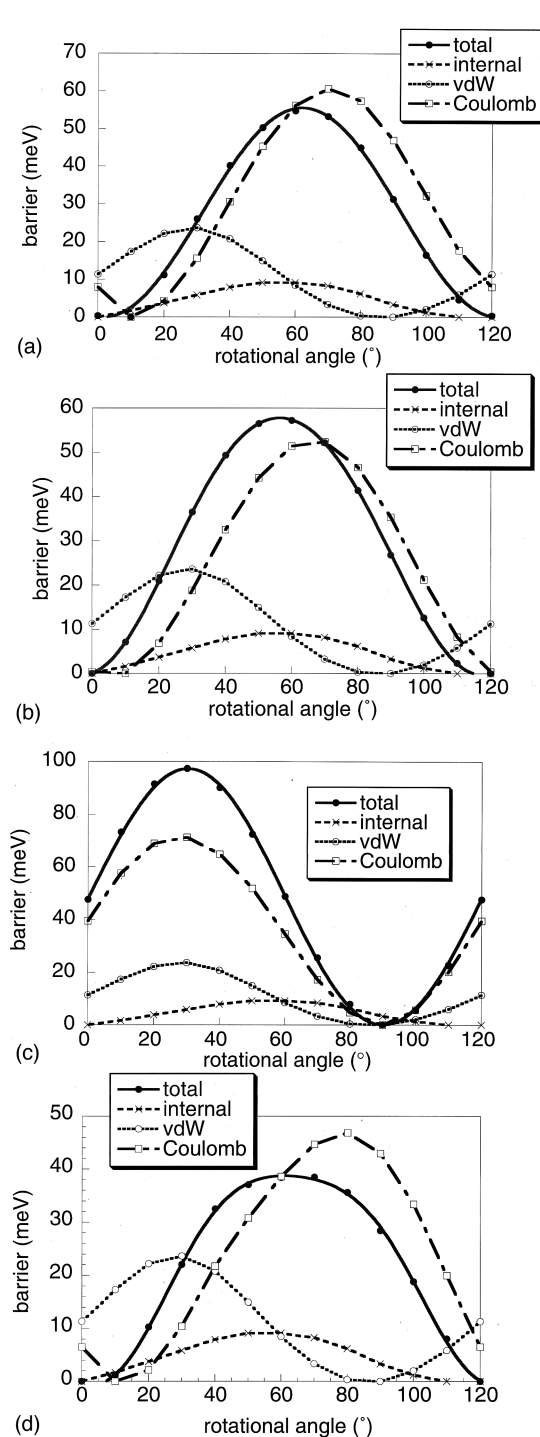


FIG. 10. Calculation of the rotational potential in cobalt acetate tetrahydrate. Total potential: solid curve with solid circle, van der Waals: dotted curve with open circle, Coulomb: dashed curve with open square, Internal: dotted curve with a cross. (a) Partial charges are calculated with the  $Q_{eq}$  method and are fixed during the rotation of the methyl group. (b) Partial charges are calculated with *ab initio* method and are fixed during the rotation of the methyl group. (c) Partial charges are calculated with the  $Q_{eq}$  method and vary during the rotation of the methyl group. (d) Partial charges are calculated with *ab initio* method and vary during the rotation of the methyl group.

method, the magnitudes being generally greater except for the hydrogen atoms.

These salts are well suited to the current investigation because, as anticipated, the Coulomb contribution dominates

TABLE V. Results of the calculations for different methods of estimating partial charges and comparison with the experimental tunneling and librational frequencies.

Nickel acetate tetrahydrate					
Fourier coeff.	Methods				
	1	2	3	4	
V3(meV)	63.2	61.1	120.2	44.4	
V6(meV)	-0.3	2.1	-0.1	6.4	
V9(meV)	0.0	0.0	0.0	0.4	
Calculated					experimental
Tunnel ( $\mu\text{eV}$ )	0.3	0.3	<0.001	1.2	1.4
Librations (meV)	17.5	18.1	24.9	16.8	15
Cobalt acetate tetrahydrate					
Fourier coeff.	Methods				
	1	2	3	4	
V3(meV)	55.5	59.7	97.3	39.2	
V6(meV)	0.5	2.6	-0.3	6.8	
V9(meV)	0.0	0.0	0.0	-0.6	
Calculated					experimental
Tunnel ( $\mu\text{eV}$ )	0.6	0.4	0.03	2.0	1.2
Librations (meV)	16.4	17.1	22.2	16.0	15

the rotational barrier, regardless of the method of calculation in every case. When using either method 1 or 2 (Figs. 9(a) and 9(b), respectively), very similar total barriers are obtained. They are almost purely three-fold with a barrier height of 63.2 and 61.1 meV, respectively. The tunnel splitting calculated from these potentials is 0.3  $\mu\text{eV}$ , which is about four times smaller than the observed value (1.4  $\mu\text{eV}$ ). Nevertheless, in both cases, the crystallographically determined orientation of the methyl group is correctly predicted to within a few degrees. In the third method [see Fig. 9(c)], the tunnel splitting is dramatically underestimated in comparison with the experiment, being calculated as less than 0.01  $\mu\text{eV}$ , and moreover, the minimum-energy orientation of the methyl group is not predicted correctly either. As one would hope, the last method, which is the most rigorous, gives the best agreement with the observables [Fig. 9(d)]. This is the method established in Ref. 12 which gives the best correlation for a series of organic molecules although in these systems the Coulomb contribution is usually the smallest of the three contributions to the rotational potential.

For the nickel salt, the calculated tunnel splitting is estimated to be 1.2  $\mu\text{eV}$  and the librations 16.8 meV, which compare very favorably with the experimental values of 1.4  $\mu\text{eV}$  and 15 meV, respectively. The Fourier coefficients are  $V_3=44.4$  meV and  $V_6=6.4$  meV. For the cobalt salt, the agreement between observed and calculated libration frequencies is also near perfect, but the tunnel frequency is a factor of 2 too high. This demonstrates the almost exponential dependence of the tunnel splitting on the barrier height, a factor of 2 corresponds to an error of less than 10% in the barrier height, which is in fact rather good agreement. The librational frequency is much less sensitive to the barrier height, and it is correspondingly easier to obtain good agreement between experimental and calculated values. These re-

sults are illustrated in Figs. 10(a)–10(d), and summarized in Table V.

We encountered a problem of convergence with the *ab initio* calculations for the cobalt salt which prevented us from estimating the potential-derived charges. The level of convergence used by default in the GAMESS-K program for nickel salt could not be attained in the cobalt salt. Reducing the convergence criterion enabled wave functions and the internal potential to be determined but the derived charges were unphysical. However, considering the proximity of cobalt and nickel in the periodic table, and that their salts are almost isostructural, we overcame this difficulty by transferring the potential-derived charges from nickel acetate tetrahydrate to cobalt acetate tetrahydrate.

### C. Other methyl dynamics

Since we now have potential parameters and partial charges which reproduce the rotational dynamics of the methyl groups, it is interesting to inquire how the observed and calculated dynamics for other degrees of freedom of the methyl group compare. This is particularly relevant because the details of the center-of-mass movement during quantum rotation of methyl groups are not well defined and could possibly entail involvement of the methyl rocking modes.

These compounds have previously been studied by IR at 300 and 95 K and Raman spectroscopy at 300 and 130 K.<sup>19,20,34</sup> The rocking mode of the methyl group was reported at 1054  $\text{cm}^{-1}$  in the both cases. A survey of the rocking frequency (out-of-plane) reveals that this mode always arises within a few wave numbers of 1055  $\text{cm}^{-1}$  regardless of the nature of the metal atom, the degree of hydration or the crystal structures.<sup>35–37</sup> The in-plane rocking mode is slightly more sensitive, varying between about 1030 and 1040  $\text{cm}^{-1}$ .

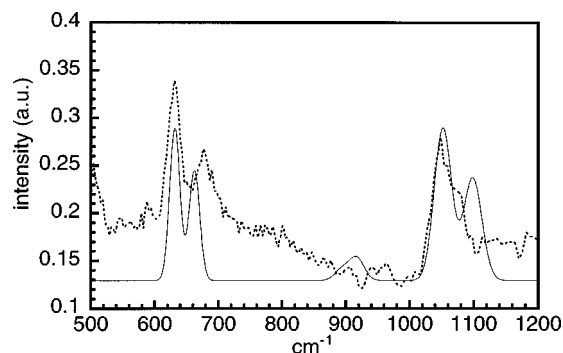


FIG. 11. Inelastic neutron scattering spectrum of  $\text{Li}(\text{CH}_3\text{COO}) \cdot 2\text{D}_2\text{O}$  measured on TFXA (dotted line) and calculated spectrum with *ab initio* method (line).

Acetate modes not involving the methyl group are much more sensitive to the crystalline environment, the  $\nu_{\text{CC}}$  mode being found between 924 and 964  $\text{cm}^{-1}$ , while the  $\nu_{\text{CO}}$  mode arises anywhere between 1408 and 1595  $\text{cm}^{-1}$ .

It has been shown that if intermolecular interactions are weak, the vibrational frequencies and amplitudes calculated by *ab initio* methods should compare well with the frequencies and intensities measured by INS.<sup>38</sup> We have recorded the INS spectrum of several metal acetates at liquid-helium temperature on the IN1 spectrometer: cobalt acetate tetrahydrate, nickel acetate tetrahydrate, zinc acetate dihydrate, and sodium acetate trihydrate. The vibrations of the water molecules dominate these spectra, but nevertheless, we can distinguish the rocking modes of the methyl group at around 1050  $\text{cm}^{-1}$  in all these spectra.

Although the resolution of the IN1 spectrometer does not allow us to separate the two methyl rocking modes in the INS spectra we have also been able to record the spectrum of  $\text{Li}(\text{CH}_3\text{COO}) \cdot 2\text{D}_2\text{O}$  using the TFXA spectrometer which has higher resolution. Because the water was deuterated for this compound, this spectrum is dominated by the vibrational modes of the methyl group, and the two rocking modes of the methyl group can be discerned as a maximum at 1050  $\text{cm}^{-1}$  with a shoulder at about 1070  $\text{cm}^{-1}$  (Fig. 11).

We performed *ab initio* calculations of the isolated acetate group  $\text{CH}_3\text{COO}^-$  with GAMESS-UK, using the 6-31G\* basis set with a complete optimized molecular geometry followed by a calculation of the harmonic frequencies. These calculations predict the frequency and the relative intensity of the rocking modes at about 1040 and 1100  $\text{cm}^{-1}$  with reasonable accuracy, a global scaling factor of 0.95 having been introduced to account for the usual overestimation of the force constants by *ab initio* methods. We have made no attempt to analyze the other parts of the vibrational spectrum as this is not of interest to the present work.

This simple model clearly shows that, at least in the acetates, the methyl rocking modes are almost purely intramolecular, any intermolecular terms being insignificant at the present level of accuracy. The picture which emerges is the acetate group, in any of its crystalline environments, being held in place by the oxygen atoms, with the methyl group seeing a rather smooth potential energy surface from its surrounding atoms.

## VIII. CONCLUSION

Rotational tunneling of the methyl group is highly sensitive to the rotational potential, but this is only a useful probe when it can be correlated with structure. The Coulomb energy in crystals of organic compounds is frequently invariant with the rotational conformation of the methyl group so that calculations which use very approximate methods to obtain the Coulomb terms give reasonable results. However, the most interesting systems are those in which the correlation between one-dimensional rotational dynamics and structure fails, since this points to novel dynamics, coupling, etc. In these circumstances, problems with Coulomb interactions need to be eliminated, or at least identified, before embarking on a time-consuming study involving additional degrees of freedom and coupling.

We have shown that point charges obtained from *ab initio* methods provide a reasonable approximation and that the best results are obtained when these are recalculated for each step in the reorientation of the methyl group. The main problem is the computational expense of this method, particularly for large models. Whereas previous calculations<sup>10-15</sup> have used a bigger basis set for the *ab initio* calculations (6-31G\*\*), this work shows that a much reduced basis set, which is imposed by the chemical composition of the system, is adequate in this case, the advantage being the reduction of the computing time.

Density functional methods (DFT) provide an accurate alternative, but these require the use of a fairly large cell to eliminate the rotation of neighboring methyl groups. With our presently available computing resources we have been unable to obtain satisfactory results for methyl dynamics in the metal acetates.

## ACKNOWLEDGMENTS

We thank M. F. Lautié from the LASIR-CNRS (Thiais, France) for providing deuterated samples of cobalt acetate. We thank P. Smith from ILL for assistance with the crystal-structure determination of cobalt acetate. We are also grateful to M. Neumann and P. Schiebel for helpful discussions.

<sup>1</sup> *Springer Tracts in Modern Physics*, edited by W. Press (Springer, Berlin, 1981).

<sup>2</sup> D. Cavagnat and M. Pesquer, *J. Chem. Phys.* **90**, 3289 (1986).

<sup>3</sup> B. M. Rice and S. F. Trevino, *J. Chem. Phys.* **94**, 1991 (1990).

<sup>4</sup> A. M. Alsaanoosi, A. J. Horsewill, and S. Clough, *J. Phys.: Condens. Matter* **1**, 643 (1989).

<sup>5</sup> A. Heidemann, M. Prager, and M. Monkenbush, *Z. Phys. B* **76**, 77 (1989).

<sup>6</sup> M. Prager, W. I. F. David, and R. M. Ibberson, *J. Chem. Phys.* **95**, 2473 (1991).

<sup>7</sup> A. M. Alsaanoosi and A. J. Horsewill, *Chem. Phys.* **160**, 25 (1992).

<sup>8</sup> J. Meinnel, M. Mani, M. Nusimovici, C. J. Carlile, B. Hennion, R. Carrier, B. Wyncke, M. Sanquer, and F. Tonnard, *Physica B* **202**, 293 (1994).

<sup>9</sup> M. Neumann and G. J. Kearley, *Chem. Phys.* **215**, 253 (1997).

<sup>10</sup> M. R. Johnson, B. Frick, and H. P. Trommsdorff, *Chem. Phys. Lett.* **187**, 258 (1996).

<sup>11</sup> M. R. Johnson, M. Neumann, B. Nicolai, P. Smith, and G. J. Kearley, *J. Chem. Phys.* **215**, 345 (1997).

<sup>12</sup> M. Neumann and M. R. Johnson, *J. Chem. Phys.* **107**, 1725 (1997).

<sup>13</sup> B. Nicolai, G. J. Kearley, O. Randl, F. Fillaux, and P. H. Trommsdorff, *Physica B* **234-236**, 76 (1997).

<sup>14</sup> B. Nicolai, E. Kaiser, F. Fillaux, G. J. Kearley, A. Cousson, and W. Paulus, *Chem. Phys.* **226**, 1 (1998).

- <sup>15</sup>P. Schiebel, G. J. Kearley, and M. R. Johnson, *J. Chem. Phys.* **108**, 2375 (1998).
- <sup>16</sup>GSAS, General Structure Analysis System, A. C. Larson, R. B. von Dreele, 1985.
- <sup>17</sup>J. N. van Niekerk and F. R. L. Schoening, *Acta Crystallogr.* **6**, 609 (1953).
- <sup>18</sup>T. C. Downi, W. Harrison, E. S. Raper, and M. A. Hepworth, *Acta Crystallogr., Sect. B: Struct. Crystallogr. Cryst. Chem.* **B27**, 706 (1971).
- <sup>19</sup>G. S. Raghuvanshi, M. Pal, M. B. Patel, and H. D. Bist, *J. Mol. Struct.* **101**, 7 (1983).
- <sup>20</sup>G. S. Raghuvanshi and H. D. Bist, *Chem. Phys. Lett.* **103**, 507 (1984).
- <sup>21</sup>G. J. Kearley, B. Nicolai, P. G. Radaelli, and F. Fillaux, *J. Solid State Chem.* **126**, 184 (1996).
- <sup>22</sup>K. Guckelsberger, H. Friedrich, and R. Scherm, *Z. Phys. B* **91**, 209 (1993).
- <sup>23</sup>S. Clough, A. Heidemann, M. N. J. Paley, and J.-B. Suck, *J. Phys. C* **13**, 6599 (1980).
- <sup>24</sup>S. A. Friedberg and J. T. Schriempf, *J. Appl. Phys.* **35**, 1000 (1964).
- <sup>25</sup>J. T. Schriempf and S. A. Friedberg, *J. Chem. Phys.* **40**, 296 (1964).
- <sup>26</sup>R. B. Flippen and S. A. Friedberg, *Phys. Rev.* **121**, 1591 (1961).
- <sup>27</sup>GAMESS-UK, Generalized atomic and molecular electronic structure system, M. F. Guest, J. Kendrick, J. H. van Lenthe, K. Schoeffel, P. Sherwood, Daresbury Laboratory, United Kingdom.
- <sup>28</sup>W. J. Hehre, L. Radom, P. R. Schleyer, and J. A. Pople, *Ab initio Molecular Orbital Theory* (Wiley-Interscience, New York, 1986).
- <sup>29</sup>A. K. Rappe, C. J. Casewitt, K. S. Colwell, W. A. Goddard, and W. M. Skiff, *J. Am. Chem. Soc.* **114**, 10024 (1992).
- <sup>30</sup>A. K. Rappe, K. S. Colwell, and C. J. Casewitt, *Inorg. Chem.* **32**, 3438 (1993).
- <sup>31</sup>N. Karasawa and W. A. Goddard, *J. Phys. Chem.* **93**, 7320 (1989).
- <sup>32</sup>CERIUS2, BIOSYM/Molecular Simulations, 9685 Scranton Road, San Diego, CA 92121-3752, 1996.
- <sup>33</sup>A. K. Rappe and W. A. Goddard, *J. Phys. Chem.* **95**, 3358 (1991).
- <sup>34</sup>G. S. Raghuvanshi, D. P. Khandelwal, and H. D. Bist, *Appl. Spectrosc.* **38**, 710 (1984).
- <sup>35</sup>G. S. Raghuvanshi, D. P. Khandelwal, and H. D. Bist, *Chem. Phys. Lett.* **93**, 371 (1982).
- <sup>36</sup>M. K. Johnson, D. B. Powell, and R. D. Cannon, *Spectrochim. Acta A* **37**, 899 (1981).
- <sup>37</sup>H. Llewellyn-Jones and E. McLaren, *J. Chem. Phys.* **22**, 1796 (1974).
- <sup>38</sup>G. J. Kearley, J. Tominson, A. Navarro, J. J. L. Gonzalez, and M. F. Gomez, *Chem. Phys.* **216**, 323 (1997).